JOURNAL OF OCULAR PHARMACOLOGY AND THERAPEUTICS
Volume 32, Number 5, 2016

DOI: 10.1089/jop.2015.0126

Differentiation of Induced Pluripotent Stem Cells to Neural Retinal Precursor Cells on Porous Poly-Lactic-co-Glycolic Acid Scaffolds

Kristan S. Worthington,[1,2] Luke A. Wiley,[1] C. Allan Guymon,[2]
Aliasger K. Salem,[3] and Budd A. Tucker[1]

Abstract

Purpose: Cell replacement therapy for the treatment of retinal degeneration is an increasingly feasible approach, but one that still requires optimization of the transplantation strategy. To this end, various polymer substrates can increase cell survival and integration, although the effect of their pore size on cell behavior, particularly differentiation, has yet to be explored.
Methods: Salt crystals of varying known size were used to impart structure to poly(lactic-co-glycolic acid) (PLGA) scaffolds by a salt leaching/solvent evaporation process. Mouse induced pluripotent stem cells (miPSCs) were seeded to the polymer scaffolds and supplemented with retinal differentiation media for up to 2 weeks. Proliferation was measured during the course of 2 weeks, while differentiation was evaluated using cell morphology and expression of early retinal development markers.
Results: The salt leaching method of porous PLGA fabrication resulted in amorphous smooth pores. Cells attached to these scaffolds and proliferated, reaching a maximum cell number at 10 days postseeding that was 5 times higher on porous PLGA than on nonporous controls. The morphology of many of these cells, including their formation of neurites, was suggestive of neural phenotypes, while their expression of Sox2, Pax6, and Otx2 indicates early retinal development.
Conclusions: The use of porous PLGA scaffolds to differentiate iPSCs to retinal phenotypes is a feasible pretransplantation approach. This adds to an important knowledge base; understanding how developing retinal cells interact with polymer substrates with varying structure is a crucial component of optimizing cell therapy strategies.

Introduction

Age-related macular degeneration, one of the leading causes of blindness in the Western world, is characterized by death of the light-sensing photoreceptor cells of the outer neural retina, the underlying retinal pigmented epithelium, and the choroidal vasculature. To restore vision to those suffering from this and similar neurodegenerative diseases, treatment beyond existing drug and/or gene augmentation approaches will be required. Many studies demonstrate the feasibility of using stem cells for photoreceptor cell replacement[1–13]; however, the development of optimal stem cell transplantation approaches is crucial. Bolus subretinal injection into hosts with end-stage disease typically results in minimal cellular survival and integration. For example, several studies have shown that as few as 0.01% and at most 5% of retinal progenitor cells (RPCs) injected into the subretinal space as a single-cell suspension survive and even fewer integrate within host retina.[1,4,9,14] These less than ideal results are due, in large part, to the lack of physical support that donor cells experience following the bolus injection.

Both degradable and nondegradable polymer scaffolds have been studied extensively as a means to provide needed support to donor cells during transplantation. For example, porous poly(lactic-co-glycolic acid) (PLGA)-based scaffolds have been shown to increase the survival and integrative capacity of RPCs following transplantation.[11,18]

[1]Department of Ophthalmology and Visual Sciences, Wynn Institute for Vision Research, The University of Iowa, Iowa City, Iowa.
[2]Department of Chemical and Biochemical Engineering, The University of Iowa, Iowa City, Iowa.
[3]Division of Pharmaceutics and Translational Therapeutics, Department of Pharmaceutical Sciences and Experimental Therapeutics, The University of Iowa, Iowa City, Iowa.

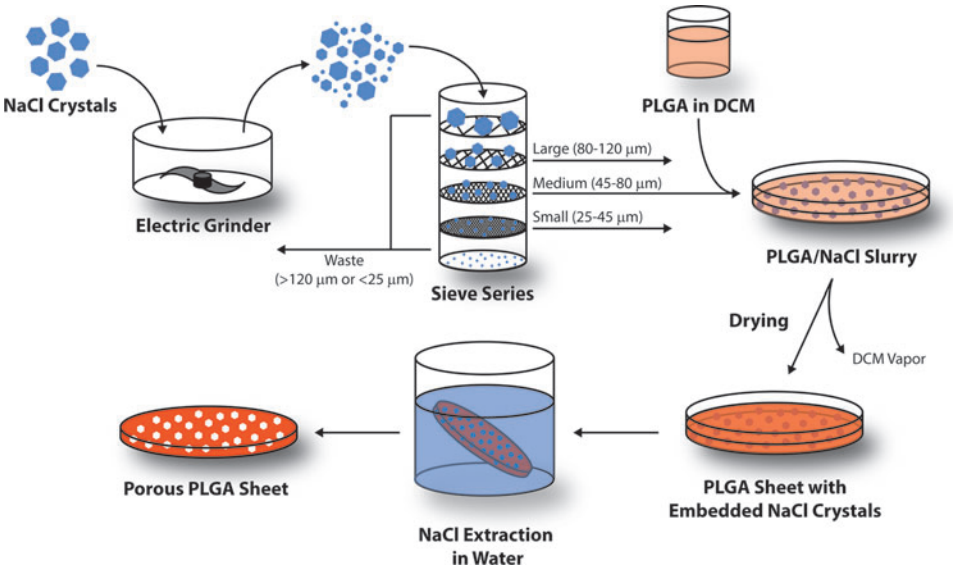

FIG. 1. Schematic of the salt leaching/solvent casting method used to fabricate poly(lactic-co-glycolic acid) (PLGA) scaffolds with various pore sizes.

Although chemical compatibility is an important and necessary focus for developing effective cell delivery scaffolds, growing evidence suggests that structural cues also play an important role in cell/biomaterial interactions. Pore size or the presence of guidance cues, for example, can help to direct both cell proliferation and differentiation. Furthermore, optimizing the porosity of a material could beneficially maximize the delivery of nutrients, oxygen, and/or water to surrounding cells and tissues. In fact, several studies have demonstrated the effects of porosity and other polymer structure on retinal cell/material interactions, including photoreceptor cell growth in grooves,[19] RPE cell growth on porous substrates,[20] and RPC growth and differentiation on porous materials.[18,21] However, to our knowledge, induced pluripotent stem cells (iPSCs) have never been differentiated toward retinal cell phenotypes on these materials, and the effects of pore size on proliferation and differentiation have yet to be characterized.

In this study, PLGA scaffolds with various pore sizes were fabricated using a simple salt leaching/solvent casting technique. The resulting materials were characterized, and the effect of pore size on iPSC proliferation and differentiation was examined.

Methods

Scaffold fabrication

Salt crystals (NaCl; Sigma-Aldrich, St. Louis, MO) were ground in an electric grinder to reduce their size and passed through a series of sieves with known mesh sizes (120, 80, 45, and 25 μm). Crystals smaller than 25 μm or larger than 120 μm were discarded, while the remaining fractions were collected and designated as small (25–45 μm), medium (45–80 μm), and large (80–120 μm). PLGA scaffolds were prepared using a standard solvent casting and particle leaching method (Fig. 1). For each size group, 800 mg of PLGA 50:50 (Resomer® RG 503; Boehringer Ingelheim KG, Ingelheim, Germany) was dissolved in 12 mL of dichloromethane (DCM). The solution was then carefully poured into a glass Petri dish containing 12 g of evenly dispersed salt crystals. PLGA sheets were also fabricated without salt (none) and with equal parts of each size of salt crystal (all).

The slurry was dried at room temperature and pressure overnight, and the resulting material was immersed in excess of distilled water to extract NaCl. This leaching process was performed for 48 h at room temperature with constant stirring and regular distilled water exchange (every 12 h). Circular punches of PLGA scaffold were created using a 5-mm biopsy punch, then sterilized by submersion in 70% ethanol, followed by thorough rinsing with sterile phosphate-buffered saline.

Cell culture

Pluripotency media comprised Dulbecco's modified Eagle's medium: Nutrient Mixture F-12 (DMEM/F12; Life Technologies, Gibco, Carlsbad, CA) with 15% fetal bovine serum (Life Technologies), 1% 100× nonessential amino acids (NEAA; Life Technologies), 0.4 mM L-glutamine (Life Technologies), 0.1 mg/mL Primocin (InvivoGen, San Diego, CA), and 8.88 ng/mL 2-mercaptoethanol (Sigma-Aldrich). Just before use, 2 U/μL of mouse recombinant leukemia inhibitory factor (mLif, ESGRO; EMD Millipore, Billerica, MA) was added and media were warmed to 37°C.

Differentiation media comprised DMEM (Life Technologies) with 2% 50× B27 supplement (Life Technologies), 1% 100× N2 supplement (Life Technologies), 0.4 mM L-glutamine (Life Technologies), 1% 100× NEAA (Life Technologies), and 0.1 mg/mL Primocin (Life Technologies). Just before use, 1 ng/mL mouse recombinant Noggin (R&D Systems, Minneapolis, MN), 1 ng/mL mouse recombinant Dkk-1 (R&D Systems), 1 ng/mL mouse recombinant Bfgf (R&D Systems), and 1 ng/mL Igf-1 (R&D Systems) were added and the media were warmed to 37°C.

Sterile PLGA scaffolds were transferred to a 96-well plate (1 sample per well) and coated with Matrigel (Corning, Corning, NY) using a thin coating method. Briefly, 1 mL Matrigel was diluted in 50 mL cold DMEM and added to the PLGA plates (200 μL/well). After 1 h at room temperature, the excess liquid was removed and cells were seeded according to the protocol below.

Previously generated dsRed mouse induced pluripotent stem cells (MiPSCs)[10,22] were used in these studies. Before beginning differentiation, MiPSCs were thawed from a frozen stock, centrifuged, resuspended in pluripotency media,

and plated on Matrigel-coated culture plates (Corning). Cells were transferred to a new plate at a density of 1:6 thrice in 1 week, with media being replaced daily. After 1 week, cells were removed from the plate using 0.25% trypsin-EDTA, washed with differentiation media, and replated on top of PLGA scaffolds at 1.5×10^4 cells/well. The differentiation media were replaced every 2 days and all cells were cultured in a humidified 37°C cell culture incubator with 5% CO_2.

Scanning electron microscopy

Samples with attached cells were fixed with glutaraldehyde, rinsed with 0.1 mM cacodylate buffer, and stained with 1% osmium tetroxide in cacodylate buffer. Samples were then washed again with cacodylate buffer and completely dried using ethanol dehydration, followed by critical point drying (E3100; Quorum Technologies, Laughton, East Sussex, England). PLGA samples without cells were examined directly after lyophilization. In either case, after drying, samples were mounted on an aluminum scanning electron microscope (SEM) stub using double-sided conductive tape. A gold–palladium coating was applied using an argon beam K550 sputter coater (Emitech Ltd., Kent, England). Images were captured using a Hitachi S-4800 SEM (Hitachi High-Technologies, Toronto, ON, Canada) at an accelerating voltage of 1 kV (without cells) or 5 kV (with cells).

Growth quantification

Cell proliferation was quantified using a colorimetric assay. As a positive control, 6 PLGA-free wells (Matrigel coated) were seeded with cells 1 day before each time point. The following day, 3 of these wells were counted by removing the cells from the plate with trypsin and using an automatic cell counter, while the remaining 3 wells were included in the MTT assay. Briefly, at the designated time point, each scaffold was transferred to a new plate and all wells were supplemented with fresh media (100 μL). MTT reagent [10 μL, 3-(4,5-dimethylthiazol-2-yl)-2,5-diphenyltetrazolium bromide; EMD Millipore] was added to each well and the plate was incubated at cell culture conditions for 4 h.

The solution was removed from each well and discarded, leaving behind insoluble MTT crystals. These crystals were dissolved by adding 100 μL of developing solution (0.04 M hydrochloric acid in isopropanol) to each well and mixed to homogeneity. Scaffolds were then removed from their wells and the light absorbance of the remaining liquid was measured at 570 nm (Tecan Infinite M200 Pro; Tecan Group Ltd., Männedorf, Switzerland).

The relative number of cells on each sample was calculated by subtracting the average absorbance for blank wells from each sample absorbance, then dividing by the average absorbance of the positive control wells, multiplying by the average number of positive control cells (as counted shortly after the reagent was added) and dividing by the initial number of cells seeded (1.5×10^4). Experiments were performed in triplicate and statistical analysis was performed using 2-way analysis of variance, followed by Tukey's *post hoc* testing.

Gene expression

RNA was isolated from cells at 7 and 14 days using an RNeasy Mini Kit (Qiagen, Venlo, Limburg, The Netherlands) and the final concentration determined using a NanoDrop 2000 spectrophotometer (Thermo Scientific, Waltham, MA). Complementary DNA (cDNA) was produced using a High-Capacity cDNA Reverse Transcriptase Kit (Applied Biosystems, Life Technologies), then genes were amplified using reverse transcriptase-PCR with (forward, reverse) primers for mouse *Sox2* (AAGGGTTCTTGCTGGGTTTT, AGACCACG AAAACGGTCTTG), *Pax6* (GGGTCTGTACCAACGATAA CAT, GGGTCCTCTCAAACTCTTTCT), and *Otx2* (GAA GGGAGAGGACGACATTTACT, AGTAGGAAGTTGAG CCAGCATAG). The resulting DNA was characterized by electrophoresis on a 2% agarose gel with a run time of 30 min.

Protein expression

After 14 days in culture, 12 samples from each group were placed directly in lysis buffer [50 mM Tris-HCl, pH 7.6, 150 mM NaCl, 10 mM CaCl2, 1% Triton X-100, 0.02% NaN3, (Sigma-Aldrich)] and incubated on ice for 1 h. As a positive control, protein was isolated in the same manner from an adult mouse retina. After centrifugation, supernatant protein concentrations were determined spectroscopically according to the manufacturer's instructions (Qubit 3.0; Life Technologies).

Protein (5 μg) from each group was subjected to sodium dodecyl sulfate–polyacrylamide gel electrophoresis (4%–20% acrylamide), transferred to PVDF, and probed with mouse anti-Sox2 (No. MAB2018; 1:1,000; R&D Systems), rabbit anti-Pax6 (No. PRB-278P; 1:1,000; BioLegend, San Diego, CA), goat biotinylated anti-Otx2 (No. BAF1979; 1:1,000; R&D Systems), and rabbit anti-β-actin (No. ab8277; 1:10,000; Abcam, Cambridge, MA). Blots were visualized with ECL reagents (GE Healthcare Life Sciences, Pittsburgh, PA) and exposed to X-ray film (Fisher Scientific, Pittsburgh, PA). X-ray films were imaged using an iPhone 6S (Apple, Cupertino, CA).

Results

As mentioned above, one of the most important design considerations when developing cell delivery scaffolds is porosity. Thus, understanding of how iPSC-derived retinal cells interact with polymer scaffolds with various pore sizes is crucial for the development of successful subretinal transplantation strategies. In this study, a salt leaching method (Fig. 1) was used to create porous PLGA scaffolds and the size and density of pores were characterized qualitatively using SEM.

As seen in Fig. 2, before being seeded with cells, salt-leached PLGA scaffolds exhibited a dense pore network with irregularly shaped pores, most of which were <10 μm in diameter. Interestingly, although the pore sizes observed using SEM were much smaller than the range of salt crystal sizes used to create them, there was a visual correlation between template size and final pore size (i.e., pore size increases from top to bottom in the top 6 panels of Fig. 2, corresponding to increasing salt crystal template size). Additionally, the scaffolds created using a blend of crystal sizes (Fig. 2G, H) did not demonstrate morphology similar to any one of the other groups, but rather appeared to have a much wider range of pore sizes, as was expected. Although the shape of the pores was consistent with salt crystal shape in a few isolated cases, generally the pores were amorphous with smooth edges.

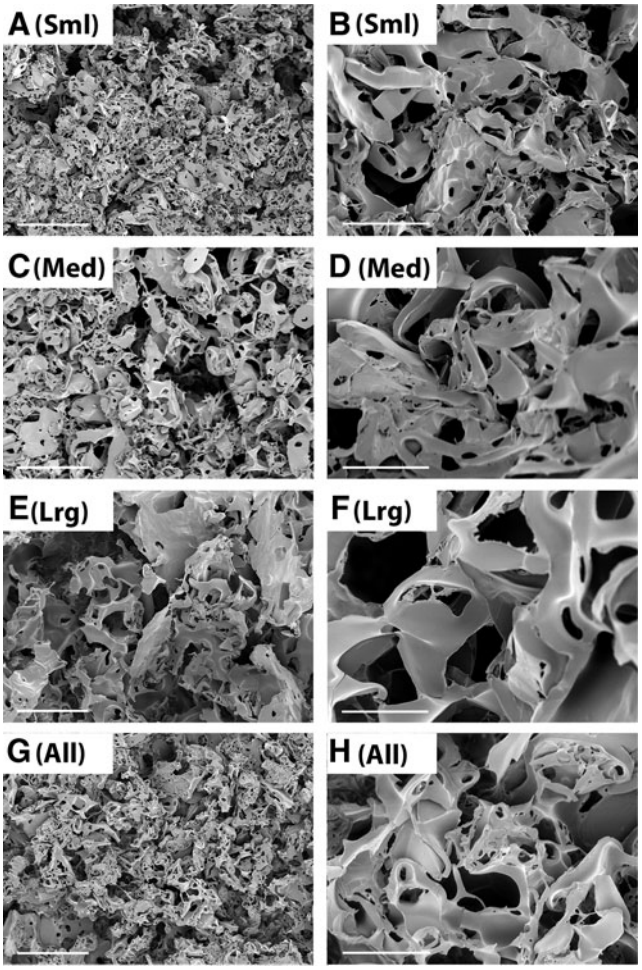

FIG. 2. Representative scanning electron microscope (SEM) images of porous PLGA. Scaffolds were fabricated with small **(A, B)**, medium **(C, D)**, large **(E, F)**, or a mixture of all sizes **(G, H)** of salt crystals. Scale bars represent 50 μm **(A, C, E, G)** or 10 μm **(B, D, F, H)**. All images were collected using an accelerating voltage of 1 kV.

All of the PLGA scaffolds examined in this study supported the attachment and growth of miPSCs for up to 2 weeks (Fig. 3A). Importantly, the inclusion of pores significantly increased the number of attached cells from 1 week postseeding onward, regardless of pore size (Fig. 3A, $^{**}P < 0.01$). Although both nonporous and porous PLGA scaffolds reached a maximum cell number at or around 10 days postseeding, nonporous PLGA scaffolds had a 6-fold increase in cell number, while the average for porous PLGA was 5 times higher at about a 25-fold increase.

As shown in Fig. 3, at 2 weeks postseeding, cells nearly covered the entire scaffold surface and integrated into the material's pores. Although in each case there were relatively few regions of the surface exposed (i.e., not covered in cells), cell morphology in these areas was also more easily characterized and thus they were selected for imaging. In all cases, cell morphology on the PLGA scaffolds was suggestive of neuronal phenotypes, as witnessed by the extensive neurite formation and branching among the cells (Fig. 3, arrowheads). In very dense areas, such as that in Fig. 3H, it appears as though the cells had formed a sheet of neurons across the entire scaffold surface. These data

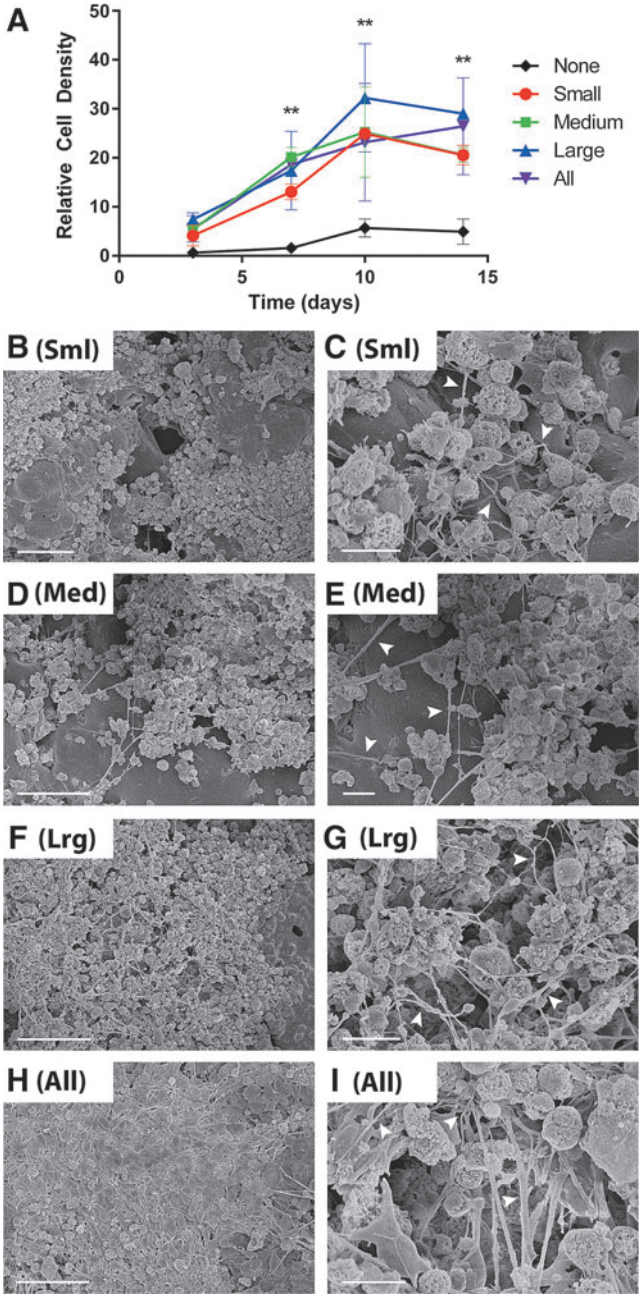

FIG. 3. Cell proliferation and differentiation on PLGA scaffolds. **(A)** Relative proliferation on porous PLGA scaffolds created using varying sizes of salt crystals was measured colorimetrically by an MTT assay at 3, 7, 10, and 14 days postseeding and compared with the number of cells seeded. Proliferation on porous samples was significantly different than nonporous controls at days 7, 10, and 14 ($^{**}P < 0.01$; exception at day 7, when small was not significantly different than nonporous; differences between porous groups were not significant). **(B–I)** Representative SEM images of induced pluripotent stem cell (iPSC)-derived cells attached to scaffolds created using small **(B, C)**, medium **(D, E)**, large **(F, G)**, or a mixture of all sizes **(H, I)** of salt crystals. Scale bars represent 50 μm **(B, D, F, H)** or 10 μm **(C, E, G, I)**. *Arrowheads* show neurite extension from cell bodies. All samples were collected 14 days postseeding and imaged at accelerating voltage of 5 kV.

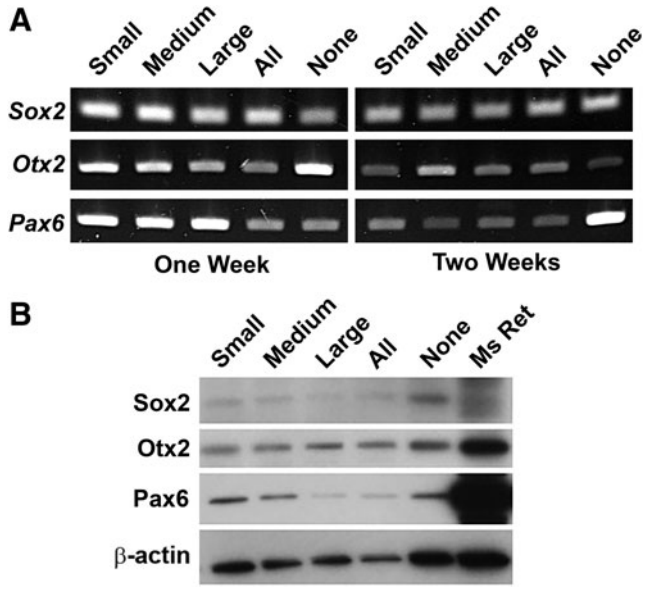

FIG. 4. Gene and protein expression of PLGA-anchored, iPSC-derived neural cells. **(A)** RNA expression of 3 early retinal markers at 1 and 2 weeks postseeding and **(B)** expression of the same 3 markers at 2 weeks postseeding compared with protein from a wild-type mouse retina suggest that attached cells have differentiated to early neural progenitor cell phenotypes.

suggest that porous PLGA scaffolds support both MiPSC proliferation and neural differentiation.

To further understand the phenotype of differentiating miPSCs attached to porous PLGA, we probed cellular gene and protein expression of Sox2, Pax6, and Otx2, each of which plays a critical role in early retinal development (Fig. 4).[23] *Sox2, Otx2, and Pax6* genes were expressed by PLGA-anchored cells at both 1 and 2 weeks postseeding, regardless of scaffold porosity (Fig. 4A). Similarly, western blotting revealed expression of Sox2, Otx2, and Pax6 in all groups and all time points tested (Fig. 4B). Interestingly, relative to their internal control (β-actin), the bands corresponding to expression of Sox2 and Otx2 in the PLGA samples appeared to be approximately equal in intensity to analogous bands in the mouse retina sample. In contrast, bands corresponding to Pax6 expression in the PLGA samples were less intense than in the mouse retina.

Discussion

In theory, by delivering cells on natural or synthetic polymer support scaffolds, the cell death associated with single cell bolus injection can be mitigated. Although several groups have investigated the use of scaffolds isolated from donor tissue, in the retina, these approaches have only been successful for RPE cells and are limited by tissue availability.[19–24] Several synthetic materials have also been investigated for the purpose of supporting replacement cells during transplantation, including inorganic materials, PMMA,[21] poly(glycerol sebecate) (PGS),[24] and poly(caprolactone) (PCL).[25] However, by far, the most commonly investigated synthetic material is PLGA. Thin, degradable PLGA scaffolds were first shown to support the growth of RPE cells nearly 20 years ago,[26] and the biomaterial interactions with retinal phenotypes have been closely studied for many years.

In addition to its ability to support both fetal and adult human RPE cells,[27–29] PLGA, when rendered porous, also supports the growth of RPCs.[18,30] In fact, when compared with bolus cell injections, transplantation of RPC-laden PLGA constructs results in 10-fold and 16-fold increases in cell survival and delivery, respectively.[18] Furthermore, micropatterned PLGA has been shown to support the growth of primary photoreceptors for a short period of time—a strong indication of its promise as a retinal cell delivery scaffold.[19]

In this work, PLGA scaffolds with randomly distributed pores were fabricated using a simple salt leaching technique. Although electrospinning, the most common PLGA processing technique, has been used extensively to create fibrous mesh scaffolds, it offers little in the way of precisely controlling pore size, as do techniques such as dioxane crystallization templating. However, the simplicity of PLGA processing using a salt leaching method, coupled with its use of readily available components and equipment, is a clear advantage for a study of this kind. Furthermore, the polydispersity of pore sizes and shapes observed in this study is likely more true to biological structures than the sometimes very uniform structures produced using other methods.

Nevertheless, there is more to be understood about the salt templating process; for example, although the presence of pores smaller than the smallest salt crystals used for templating could be due to inefficient sieving, it is unlikely that fine grain contamination would occur with such great prevalence. Furthermore, given the cuboidal shape of salt crystals, a true 1:1 transfer of structure from the crystalline template to the PLGA void spaces would not result in the smooth amorphous pores observed in this study. Rather, in addition to the size of the salt crystals, the final PLGA structure is likely affected by PLGA network shrinkage during drying and salt extraction, as well as the formation of salt water channels that form as salt diffuses away from the scaffold.

Although degradation was not addressed in this study, we speculate that larger salt template sizes lead to a greater number and volume of interconnected pores that increase surface area, facilitate transport within the scaffold and thus speed degradation. Therefore, this simple method for tuning pore size may be a useful tool with which to tune scaffold degradation rate, helping to hedge against unwanted accumulation of acidic by products in the sub-retinal space. The degradation behavior of porous scaffolds as a function of template size, along with the relationship between original template and final structure, merit further investigation in future studies.

In addition to scaffold design, selection of the appropriate cell type will likely be critical to the success of any cell replacement strategy. Since autologous cells are less likely to elicit an immune response than allogeneic donor cells following subretinal transplantation, patient-specific iPSCs are an attractive alternative. Immunological matching will be especially important for those suffering from advanced blindness, which typically involves extensive damage to the outer neural retinal, underlying RPE, and choroidal vasculature. However, cultivating and maintaining autologous cells under the appropriate conditions for human transplantation (i.e., using xeno-free media in an FDA-sanctioned good manufacturing practice facility) are far from inexpensive, so appropriately managing time and resources must go hand in hand with maximizing treatment efficiency.

Thus, the ability of cell delivery scaffolds to promote cellular proliferation and differentiation is important. In this study, we observed a 5-fold increase ($P < 0.01$) in the maximum number of cells attached to porous PLGA scaffolds over their nonporous counterparts, suggesting, as others have in the past, the importance of polymer porosity for cellular delivery.

That said, to maximize cell delivery using this approach, one would want to ensure cessation of proliferation and complete scaffold coverage prior to transplantation. However, at this and longer time points, the cell density is still an order of magnitude lower than that of photoreceptor cells in the macula. Thus, in order to truly achieve the packing necessary to recapitulate the macula, materials with precisely controlled, 3D architecture will likely be needed. Still, differentiation of iPSCs directly on their intended implantable substrate rather than dissociating and seeding onto a scaffold after differentiation could help retain desired morphologies and extracellular matrix. As cells differentiate and exit the cell cycle, their dissociation becomes increasingly detrimental to normal cellular processes and morphology. Thus, differentiating on the transplantation substrate could make for a more efficient and effective pretransplantation strategy.

Additionally, differentiating attached cells *in vitro* could provide insight into cell fate after implantation and subjection to the subretinal environment. We demonstrated that porous PLGA scaffolds adequately support the differentiation of stem cells to neural phenotypes, as confirmed morphologically, and to early retinal phenotypes, as confirmed biochemically. Taken together, the results presented here suggest that differentiating iPSCs to retinal phenotypes on a polymer substrate before implantation may be a viable strategy, although a thorough analysis and quantification of differentiation should be performed before *in vivo* experiments.

To this end, future studies should focus on comparing at least 3 pretransplantation approaches *in vitro*: the approach described here (seed with iPSCs and begin differentiation immediately), seeding with iPSCs and beginning differentiation once maximum cell number has been achieved, and differentiating cells traditionally before transferring them to the material. Cell fate and longevity under these 3 separate conditions and at longer differentiation time points should be examined to identify a transplantation strategy that truly optimizes the delivery of a large number of cells of the appropriate phenotype.

Acknowledgments

The authors gratefully acknowledge financial support from the National Institutes of Health (1 R01 024605–01, 1 DP2 OD007483-01) and the Stephen A. Wynn Institute for Vision Research. Scanning electron microscopy (NIH Shared Instrumentation Grant 1 S10 RR022498-01) was performed in the University of Iowa Central Microscopy Facility, a core resource supported by the Vice President for Research and Economic Development, the Holden Comprehensive Cancer Center, and the Carver College of Medicine. Special thanks to Chantal Allamargot for her assistance and instruction regarding SEM preparation of biological samples.

Author Disclosure Statement

No competing financial interests exist.

References

1. Barber, A.C., Hippert, C., Duran, Y., West, E.L., Bainbridge, J.W., Warre-Cornish, K., Luhmann, U.F., Lakowski, J., Sowden, J.C., Ali, R.R., and Pearson, R.A. Repair of the degenerate retina by photoreceptor transplantation. *Proc. Natl. Acad. Sci. U. S. A*. 110:354–359, 2013.
2. Gonzalez-Cordero, A., West, E.L., Pearson, R.A., Duran, Y., Carvalho, L.S., Chu, C.J., Naeem, A., Blackford, S.J., Georgiadis, A., Lakowski, J., Hubank, M., Smith, A.J., Bainbridge, J.W., Sowden, J.C., and Ali, R.R. Photoreceptor precursors derived from three-dimensional embryonic stem cell cultures integrate and mature within adult degenerate retina. *Nat. Biotechnol*. 31:741–747, 2013.
3. Gust, J., and Reh, T.A. Adult donor rod photoreceptors integrate into the mature mouse retina. *Invest. Ophthalmol. Vis. Sci*. 52:5266–5272, 2011.
4. Klassen, H., Sakaguchi, D.S., and Young, M.J. Stem cells and retinal repair. *Prog. Retin. Eye Res*. 23:149–181, 2004.
5. La Torre, A., Lamba, D.A., Jayabalu, A., and Reh, T.A. Production and transplantation of retinal cells from human and mouse embryonic stem cells. *Methods Mol. Biol*. 884:229–246, 2012.
6. Lakowski, J., Han, Y.T., Pearson, R.A., Gonzalez-Cordero, A., West, E.L., Gualdoni, S., Barber, A.C., Hubank, M., Ali, R.R., and Sowden, J.C. Effective transplantation of photoreceptor precursor cells selected via cell surface antigen expression. *Stem Cells*. 29:1391–1404, 2011.
7. Lamba, D.A., Gust, J., and Reh, T.A. Transplantation of human embryonic stem cell-derived photoreceptors restores some visual function in Crx-deficient mice. *Cell Stem Cell*. 4:73–79, 2009.
8. Ma, J., Kabiel, M., Tucker, B.A., Ge, J., and Young, M.J. Combining chondroitinase ABC and growth factors promotes the integration of murine retinal progenitor cells transplanted into Rho(-/-) mice. *Mol. Vis*. 17:1759–1770, 2011.
9. MacLaren, R.E., Pearson, R.A., MacNeil, A., Douglas, R.H., Salt, T.E., Akimoto, M., Swaroop, A., Sowden, J.C., and Ali, R.R. Retinal repair by transplantation of photoreceptor precursors. *Nature*. 444:203–207, 2006.
10. Tucker, B.A., Mullins, R.F., Streb, L.M., Anfinson, K., Eyestone, M.E., Kaalberg, E., Riker, M.J., Drack, A.V., Braun, T.A., and Stone, E.M. Patient-specific iPSC-derived photoreceptor precursor cells as a means to investigate retinitis pigmentosa. *eLife*. 2:e00824, 2013.
11. Tucker, B.A., Redenti, S.M., Jiang, C., Swift, J.S., Klassen, H.J., Smith, M.E., Wnek, G.E., and Young, M.J. The use of progenitor cell/biodegradable MMP2-PLGA polymer constructs to enhance cellular integration and retinal repopulation. *Biomaterials*. 31:9–19, 2010.
12. West, E.L., Gonzalez-Cordero, A., Hippert, C., Osakada, F., Martinez-Barbera, J.P., Pearson, R.A., Sowden, J.C., Takahashi, M., and Ali, R.R. Defining the integration capacity of embryonic stem cell-derived photoreceptor precursors. *Stem Cells*. 30:1424–1435, 2012.
13. Yao, J., Tucker, B.A., Zhang, X., Checa-Casalengua, P., Herrero-Vanrell, R., and Young, M.J. Robust cell integration from co-transplantation of biodegradable MMP2-PLGA microspheres with retinal progenitor cells. *Biomaterials*. 32:1041–1050, 2011.
14. Ballios, B.G., Cooke, M.J., Donaldson, L., Coles, B.L., Morshead, C.M., van der Kooy, D., and Shoichet, M.S. A hyaluronan-based injectable hydrogel improves the survival and integration of stem cell progeny following transplantation. *Stem Cell Reports*. 4:1031–1045, 2015.

15. Lu, B., Zhu, D., Hinton, D., Humayun, M.S., and Tai, Y.C. Mesh-supported submicron parylene-C membranes for culturing retinal pigment epithelial cells. *Biomed. Microdevices*. 14:659–667, 2012.
16. Ribeiro, R.M., Oregon, A., Diniz, B., Fernandes, R.B., Koss, M.J., Charafeddin, W., Hu, Y., Thomas, P., Thomas, B.B., Maia, M., Chader, G.J., Hinton, D.R., and Humayun, M.S. In vivo detection of hESC-RPE cells via confocal near-infrared fundus reflectance. *Ophthalmic Surg. Lasers Imaging Retina*. 44:380–384, 2013.
17. Diniz, B., Thomas, P., Thomas, B., Ribeiro, R., Hu, Y., Brant, R., Ahuja, A., Zhu, D., Liu, L., Koss, M., Maia, M., Chader, G., Hinton, D.R., and Humayun, M.S. Subretinal implantation of retinal pigment epithelial cells derived from human embryonic stem cells: improved survival when implanted as a monolayer. *Invest. Ophthalmol. Vis. Sci*. 54:5087–5096, 2013.
18. Tomita, M., Lavik, E., Klassen, H., Zahir, T., Langer, R., and Young, M.J. Biodegradable polymer composite grafts promote the survival and differentiation of retinal progenitor cells. *Stem Cells*. 23:1579–1588, 2005.
19. Tezcaner, A., and Hicks, D. In vitro characterization of micropatterned PLGA-PHBV8 blend films as temporary scaffolds for photoreceptor cells. *J. Biomed. Mater. Res. A*. 86:170–181, 2008.
20. Lim, J.M., Byun, S., Chung, S., Park, T.H., Seo, J.M., Joo, C.K., Chung, H., and Cho, D.I. Retinal pigment epithelial cell behavior is modulated by alterations in focal cell-substrate contacts. *Invest. Ophthalmol. Vis. Sci*. 45:4210–4216, 2004.
21. Tao, S., Young, C., Redenti, S., Zhang, Y., Klassen, H., Desai, T., and Young, M.J. Survival, migration and differentiation of retinal progenitor cells transplanted on micro-machined poly(methyl methacrylate) scaffolds to the subretinal space. *Lab Chip*. 7:695–701, 2007.
22. Tucker, B.A., Anfinson, K.R., Mullins, R.F., Stone, E.M., and Young, M.J. Use of a synthetic xeno-free culture substrate for induced pluripotent stem cell induction and retinal differentiation. *Stem Cells Transl. Med*. 2:16–24, 2013.
23. Hever, A.M., Williamson, K.A., and van Heyningen, V. Developmental malformations of the eye: the role of PAX6, SOX2 and OTX2. *Clin. Genet*. 69:459–470, 2006.
24. Neeley, W.L., Redenti, S., Klassen, H., Tao, S., Desai, T., Young, M.J., and Langer, R. A microfabricated scaffold for retinal progenitor cell grafting. *Biomaterials*. 29:418–426, 2008.
25. McHugh, K.J., Tao, S.L., and Saint-Geniez, M. Porous poly(epsilon-caprolactone) scaffolds for retinal pigment epithelium transplantation. *Invest. Ophthalmol. Vis. Sci*. 55:1754–1762, 2014.
26. Lu, L., Garcia, C.A., and Mikos, A.G. Retinal pigment epithelium cell culture on thin biodegradable poly(DL-lactic-co-glycolic acid) films. *J. Biomater. Sci. Polym. Ed*. 9:1187–1205, 1998.
27. Giordano, G.G., Thomson, R.C., Ishaug, S.L., Mikos, A.G., Cumber, S., Garcia, C.A., and Lahiri-Munir, D. Retinal pigment epithelium cells cultured on synthetic biodegradable polymers. *J. Biomed. Mater. Res*. 34:87–93, 1997.
28. Lu, L., Yaszemski, M.J., and Mikos, A.G. Retinal pigment epithelium engineering using synthetic biodegradable polymers. *Biomaterials*. 22:3345–3355, 2001.
29. Hadlock, T., Singh, S., Vacanti, J.P., and McLaughlin, B.J. Ocular cell monolayers cultured on biodegradable substrates. *Tissue Eng*. 5:187–196, 1999.
30. Lavik, E.B., Klassen, H., Warfvinge, K., Langer, R., and Young, M.J. Fabrication of degradable polymer scaffolds to direct the integration and differentiation of retinal progenitors. *Biomaterials*. 26:3187–3196, 2005.

Received: September 22, 2015
Accepted: November 24, 2015

Address correspondence to:
Dr. Budd A. Tucker
Department of Ophthalmology and Visual Sciences
Wynn Institute for Vision Research
The University of Iowa
Iowa City, IA 52240

E-mail: budd-tucker@uiowa.edu